1-kV Sputtered p-NiO/n-Ga_2O_3 Heterojunction Diodes With an Ultra-Low Leakage Current Below 1 μA/cm^2

Xing Lu, *Member, IEEE*, Xianda Zhou, *Member, IEEE*, Huaxing Jiang, *Member, IEEE*, Kar Wei Ng, Zimin Chen, Yanli Pei, Kei May Lau, *Life Fellow, IEEE*, and Gang Wang

***Abstract*— High performance NiO/β-Ga_2O_3 heterojunction pn diodes were realized by applying a sputtered p-type NiO film onto a lightly doped n-type β-Ga_2O_3 epitaxial layer. Taking advantage of the high barrier height against carriers within the pn heterojunction, the demonstrated device exhibited a high breakdown voltage (V_B) of 1059 V without optimized electric field management techniques, and before breakdown the reverse leakage current density remained below 1 μA/cm^2. Simultaneously, a relatively low specific on-resistance ($R_{on,sp}$) of 3.5 m$\Omega\cdot cm^2$ was achieved. The built-in potential of the heterojunction that determined by a capacitance-voltage (*C-V*) measurement was around 2.4 eV. As discussed in terms of the energy band diagram of a type-II heterojunction, the conduction band and valence band offsets at the NiO/β-Ga_2O_3 hetero-interface were estimated to be 1.2 and 2.3 eV, respectively.**

***Index Terms*— β-Ga_2O_3, breakdown voltage, heterojunction, NiO, p-n diode, reverse leakage current.**

I. Introduction

GALLIUM Oxide (Ga_2O_3) semiconductor has attracted great attention in developing next generation high-voltage power electronics owing to its ultra-wide bandgap of around 4.8 eV and high breakdown electric field (E_C) [1], [2]. The theoretical E_C of Ga_2O_3 is expected to exceed 8 MV/cm, more than double that of SiC and GaN, which translates to far superior power device performance predicted by the Baliga's figure-of-merit (*BFoM*) [3], [4]. Moreover, advances in single crystalline β-Ga_2O_3 substrate synthesis, especially by the cost-competitive melt growth methods [5]–[9], provide great benefits for the development of Ga_2O_3-based high-voltage power devices with a vertical geometry. Due to the high current handling capability, a vertical device is highly desirable for most applications. In recent years, high breakdown voltages (V_B) exceeding 2 kV have been achieved in β-Ga_2O_3 Schottky barrier diodes (SBDs) [10]–[14], while most of which had a relatively high leakage current density exceeding mA/cm^2 at a high reverse bias level. On the other hand, β-Ga_2O_3-based vertical trench SBDs with high V_B and low reverse leakage current were demonstrated [15, 16], where the advanced Ga_2O_3 etching techniques have to be employed.

Although the great progress in unipolar devices has been made, the absence of p-type doping capability remains a major limitation to Ga_2O_3-based power electrons. The widely used bipolar structures and junction-based edge termination schemes in the commercialized Si and SiC power electronics are quite challenging for Ga_2O_3-based devices [17]. One possible solution is to construct p-n heterojunctions by employing other p-type materials [18]–[21]. By sputtering p-Cu_2O on a 10 μm epitaxial n^--β-Ga_2O_3 drift layer, 1.49-kV vertical heterojunction diodes have been realized, while the potential of such device might be limited by the much narrower bandgap of p-Cu_2O [19]. p-NiO/n-Ga_2O_3 heterojunction diodes have also been reported, but the V_B was relatively compromised [20], [21].

In this work, we demonstrated high performance vertical NiO/β-Ga_2O_3 heterojunction p-n diodes by sputtering a layer of p-NiO on an epitaxial n^--β-Ga_2O_3 layer. A low specific on-resistance ($R_{on,sp}$) of 3.5 m$\Omega\cdot cm^2$ and high V_B of 1059 V were achieved simultaneously. Before breakdown the heterojunction diodes exhibited an ultra-low reverse leakage current density of below 1 μA/cm^2. The results pave the way for the development of NiO/β-Ga_2O_3 heterojunction for future high-voltage power electronics.

II. Device Structure and Fabrication

Fig. 1(a) schematically illustrates the device structures of the vertical NiO/β-Ga_2O_3 heterojunction p-n diode and the Ni/β-Ga_2O_3 SBD fabricated on the same sample. An 8-μm lightly doped n-type β-Ga_2O_3 drift layer was grown on a conductive bulk (001) β-Ga_2O_3 substrate. Prior to the device fabrication, the sample was cleaned with acetone and isopropanol, followed by a 4-cycle deionized (DI) water rinse. After cleaning, Ohmic metal was deposited on back side of the sample by blanket evaporation of Ti/Al/Ti/Au

Manuscript received December 27, 2019; accepted January 14, 2020. Date of publication January 17, 2020; date of current version February 25, 2020. This work was supported in part by the Guangdong Basic and Applied Basic Research Foundation under Grant No. 2019A1515012160 and the SYSU Fundamental Research Funds for the Central Universities under Grant No. 191gpy83. The review of this letter was arranged by Editor D. G. Senesky. *(Corresponding authors: Xing Lu; Xianda Zhou.)*

Xing Lu, Xianda Zhou, Zimin Chen, Yanli Pei, and Gang Wang are with the State Key Laboratory of Optoelectronic Materials and Technologies, School of Electronics and Information Technology, Sun Yat-sen University, Guangzhou 510275, China (e-mail: lux86@mail.sysu.edu.cn; zhouxianda@mail.sysu.edu.cn).

Huaxing Jiang and Kei May Lau are with the Department of Electronic and Computer Engineering, The Hong Kong University of Science and Technology, Hong Kong.

Kar Wei Ng is with the Institute of Applied Physics and Materials Engineering, University of Macau, Taipa, Macau.

Color versions of one or more of the figures in this letter are available online at http://ieeexplore.ieee.org.

Digital Object Identifier 10.1109/LED.2020.2967418

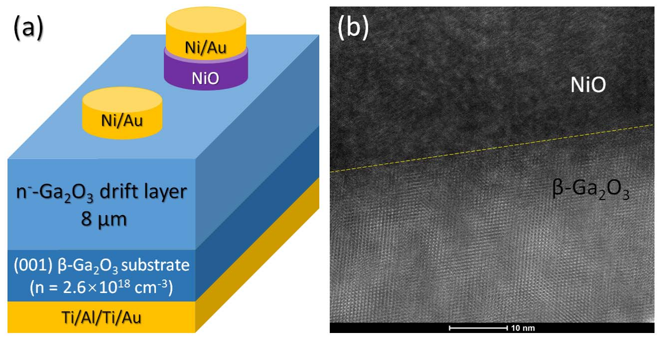

Fig. 1. (a) Schematic device structures of the vertical NiO/β-Ga_2O_3 heterojunction p-n diode and the Ni/β-Ga_2O_3 SBD fabricated on a bulk β-Ga_2O_3 substrate, (b) cross sectional TEM image showing the hetero-interface between NiO and β-Ga_2O_3.

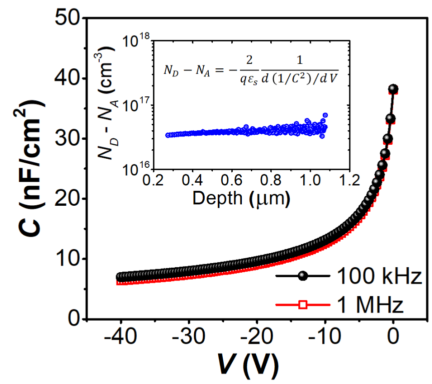

Fig. 2. *C-V* measurement performed on the fabricated Ni/β-Ga_2O_3 SBDs at 100 kHz and 1 MHz. Inset: Net doping concentration ($N_D - N_A$) in the epitaxial β-Ga_2O_3 drift layer extracted from the *C-V* measurement.

(20/150/50/80 nm). Then, 200 nm NiO was sputtered from a NiO target onto the front side of the sample and patterned using a lift-off process. The sputtering process was performed at room temperature and in a mixture of Ar/O_2 (15/5 sccm) ambient with a chamber pressure of 3 mTorr and a radio-frequency (RF) power of 150 W. The deposition rate of the NiO is 0.75 nm/min. Finally, the anode electrodes for the heterojunction diodes and the SBDs were formed by e-beam evaporation of a Ni/Au (50/100 nm) metal stack. The anode electrodes for both diodes were circular in shape with a diameter of 200 μm. Fig. 1(b) shows the high-resolution cross sectional Transmission Electron Microscopy (TEM) image of the NiO/β-Ga_2O_3 heterojunction. It can be observed that the sputtered NiO is polycrystalline and the hetero-interface exhibits excellent abruptness. The quality of the hetero-interface has profound impact on the electrical properties of the heterojunction diodes.

To evaluate the properties of the sputtered NiO, a layer of 200 nm NiO was deposited on a double polished sapphire substrate using the same deposition condition as in the device fabrication process for optical absorption and Hall measurements. The NiO showed an optical bandgap of $\sim$ 3.7 eV. A clear p-type conductivity was obtained with a relatively high hole concentration of around 1×10^{19} cm^{-3} and a low hall mobility of 0.24 cm^2/V·s, although no intentionally doping was adopted to the NiO film. The high hole concentration mainly arises from the formation of intrinsic defects like nickel vacancies which convert nearby Ni^{2+} ions into Ni^{3+}, each ion contributing an extra hole to the system [22]. The low hole mobility is due to the formation of polarons through a local distortion of the lattice around the Ni^{3+} sites, where the holes are strongly localized and can only move through the crystal by a thermally activated hopping process.

III. Results and Discussion

Fig. 2 shows the capacitance-voltage (C-V) measurement that performed on the fabricated Ni/β-Ga_2O_3 SBD at 100 kHz and 1 MHz. The net doping concentration ($N_D - N_A$) in the epitaxial β-Ga_2O_3 drift layer was extracted to be around 4×10^{16} cm^{-3} (inset of Fig. 2) according to

$$N_D - N_A = -\frac{2}{q\varepsilon_s}\frac{1}{d\left(1/C^2\right)/dV}$$

where N_D, N_A, q and ε_s are donor and acceptor concentrations in the β-Ga_2O_3 substrate, the electron charge and the

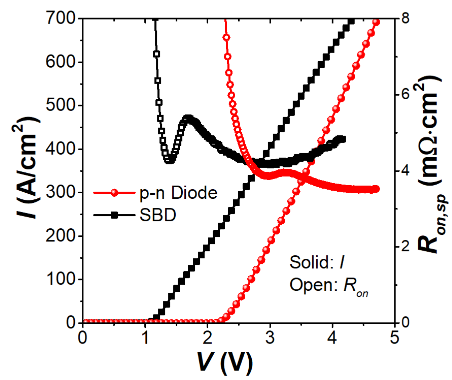

Fig. 3. Comparison of the forward *I-V* curves for the fabricated NiO/β-Ga_2O_3 heterojunction p-n diodes and Ni/β-Ga_2O_3 SBDs in a linear scale.

permittivity of β-Ga_2O_3, respectively. The Schottky barrier height extracted from the C-V measurement was around 1.3 V, in agreement with the reported results in the literature.

The linear plots of the forward current-voltage (I-V) curves for the fabricated vertical NiO/β-Ga_2O_3 heterojunction p-n diode and Ni/β-Ga_2O_3 SBD are shown in Fig. 3. The turn-on voltage (V_{on}) for the SBD was extracted to be around 1.2 V, in good agreement with the reported results for β-Ga_2O_3 SBDs in the literatures [10]–[14]. On the other hand, the NiO/β-Ga_2O_3 heterojunction p-n diode had a V_{on} of around 2.4 V, which means a higher barrier height against carriers. Fig. 3 also compares the $R_{on,sp}$ of the two fabricated devices. Obviously, the NiO/β-Ga_2O_3 heterojunction p-n diode exhibited a lower $R_{on,sp}$ (3.5 $m\Omega \cdot cm^2$) than the Ni/β-Ga_2O_3 SBD (4.2 $m\Omega \cdot cm^2$). Fig. 4 shows temperature dependent forward I-V characteristics of the NiO/β-Ga_2O_3 heterojunction p-n diode in a semi-log scale. The obtained ideality factor values were 1.22$\sim$1.57 at elevated temperatures up to 125°, suggesting a participation of the interface recombination mechanism in the forward conduction of the device [23]. Since recombination centers likely exist at the NiO/β-Ga_2O_3 hetero-interface, it is highly possible that large amount of electrons and holes recombines at interface during the device forward bias, resulting in a high forward current and low $R_{on,sp}$.

Fig. 5 shows the breakdown characteristics of the fabricated vertical NiO/β-Ga_2O_3 heterojunction p-n diode and Ni/β-Ga_2O_3 SBD. Compared to the SBD with a V_B

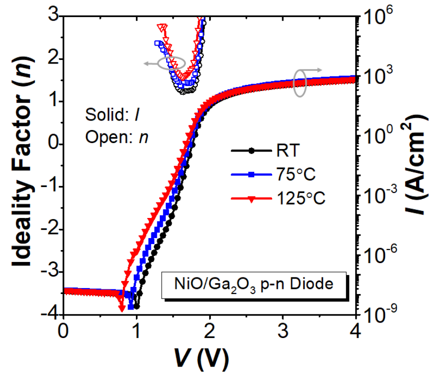

Fig. 4. Temperature dependent forward *I-V* characteristics and ideality factors of the NiO/β-Ga_2O_3 heterojunction p-n diode.

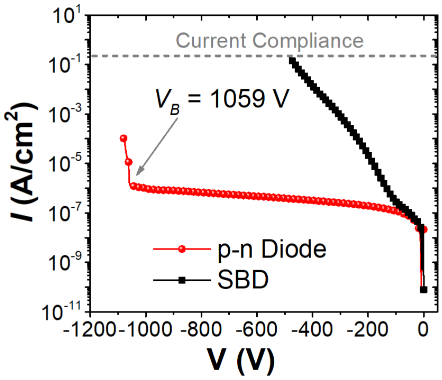

Fig. 5. Comparison of the breakdown characteristics for the fabricated vertical NiO/β-Ga_2O_3 heterojunction p-n diode and Ni/β-Ga_2O_3 SBD.

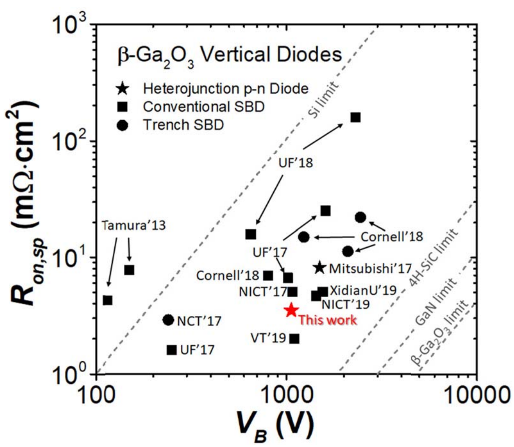

Fig. 6. Benchmark of $R_{on,\,sp}$ vs. V_B of NiO/β-Ga_2O_3 heterojunction diodes in this work and the previously reported vertical β-Ga_2O_3 diodes.

of $\sim$ 500 V, the heterojunction p-n diode yielded a much higher V_B of 1059 V and an ultra-low reverse leakage current density below 1 μA/cm^2 before breakdown, without any optimized electric field management techniques. Low reverse leakage current is a critical factor for the realization of high-efficiency power rectifiers. Based on one-dimensional Poisson's equation ($E_{peak}^{ave} \approx \sqrt{2qN_DV_B}/\varepsilon$ and $W \approx \varepsilon E_{peak}/qN_D$), the averaged peak E-field (E_{peak}^{ave}) at the heterojunction and the depletion depth (W) within β-Ga_2O_3 were calculated to be $\sim$ 3.9 MV/cm and $\sim$ 5.4 μm, respectively. Fig. 6 benchmarks the $R_{on,sp}$ vs. V_B of our NiO/β-Ga_2O_3 heterojunction p-n diode with the other state-of-the-art vertical β-Ga_2O_3 power diodes.

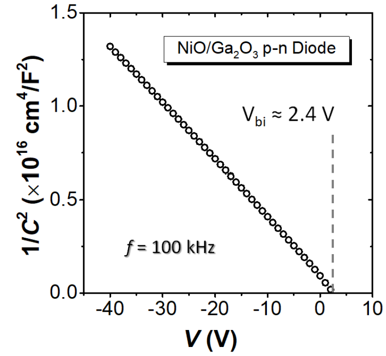

Fig. 7. 1/C^2 plot for the NiO/β-Ga_2O_3 heterojunction p-n diode. The V_{bi} is extracted to be $\sim$ 2.4 V.

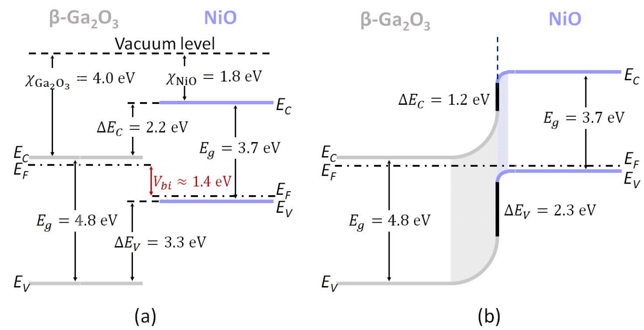

Fig. 8. The (a) theoretically estimated and (b) experimental schematic energy band diagrams of the NiO/β-Ga_2O_3 heterojunction.

Based on the difference in the electron affnities of isolated NiO and β-Ga_2O_3, the conduction band offset (ΔE_C) between NiO and β-Ga_2O_3 was estimated to be 2.2 eV. Accordingly, the valence band offset (ΔE_V) should be 3.3 eV based on the bandgap values of NiO and β-Ga_2O_3, which are 3.7 and 4.8 eV, respectively. As a result, a type-II band alignment occurred at the NiO/β-Ga_2O_3 hetero-interface [21] and the built-in potential should be around 1.4 eV, as illustrated in Fig. 8(a). However, the *C-V* measurement results did not match with the assumption made from bulk material properties. As shown in Fig. 7, the V_{bi} of the NiO/β-Ga_2O_3 heterojunction diode in our study is extracted to be around 2.4 V. Therefore, the ΔE_C and ΔE_V are $\sim$ 1.2 and 2.3 eV, respectively, much smaller than the above estimation. Fig. 8 schematically compares the theoretically estimated and the experimental energy band diagrams of the NiO/β-Ga_2O_3 heterojunction p-n diodes in our study. The difference between our experimental results and the estimation from the bulk properties maybe due to the different crystal structures (polycrystalline NiO in our experiments).

IV. Conclusion

By sputtering a p-type NiO thin film on an n-type β-Ga_2O_3 epitaxial layer, high performance vertical NiO/β-Ga_2O_3 heterojunction p-n diodes were realized. Compared to the Ni/β-Ga_2O_3 SBDs fabricated on the same sample, greatly enhanced reverse blocking characteristics were achieved, including a high V_B of 1059V and an ultra-low reverse leakage current of below 1 μA/cm^2 before breakdown. In addition, a relatively low $R_{on,sp}$ of 3.5 m$\Omega \cdot$cm^2 was maintained. These results demonstrated the high quality of the p-NiO/n-Ga_2O_3 heterojunction and its great potential for β-Ga_2O_3-based power electronics.

References

[1] M. Higashiwaki, K. Sasaki, A. Kuramata, T. Masui, and S. Yamakoshi, "Development of gallium oxide power devices," *Phys. Status Solidi A*, vol. 211, no. 1, pp. 21–26, Jan. 2014, doi: 10.1002/pssa.201330197.

[2] M. Higashiwaki and G. H. Jessen, "Guest editorial: The dawn of gallium oxide microelectronics," *Appl. Phys. Lett.*, vol. 112, no. 6, Feb. 2018, Art. no. 060401, doi: 10.1063/1.5017845.

[3] T. P. Chow, I. Omura, M. Higashiwaki, H. Kawarada, and V. Pala, "Smart power devices and ICs using GaAs and wide and extreme bandgap semiconductors," *IEEE Trans. Electron Devices*, vol. 64, no. 3, pp. 856–873, Mar. 2017, doi: 10.1109/ted.2017.2653759.

[4] B. Baliga, "Power semiconductor device figure of merit for high-frequency applications," *IEEE Electron Device Lett.*, vol. 10, no. 10, pp. 455–457, Oct. 1989, doi: 10.1109/55.43098.

[5] E. G. Víllora, K. Shimamura, Y. Yoshikawa, K. Aoki, and N. Ichinose, "Large-size β-Ga_2O_3 single crystals and wafers," *J. Cryst. Growth*, vol. 270, nos. 3–4, pp. 420–426, Oct. 2004, doi: 10.1016/j.jcrysgro.2004.06.027.

[6] Y. Tomm, P. Reiche, D. Klimm, and T. Fukuda, "Czochralski grown Ga_2O_3 crystals," *J. Cryst. Growth*, vol. 220, no. 4, pp. 510–514, Dec. 2000, doi: 10.1016/s0022-0248(00)00851-4.

[7] Z. Galazka, R. Uecker, D. Klimm, K. Irmscher, M. Naumann, M. Pietsch, A. Kwasniewski, R. Bertram, S. Ganschow, and M. Bickermann, "Scaling-up of bulk β-Ga_2O_3 single crystals by the Czochralski method," *ECS J. Solid State Sci. Technol.*, vol. 6, pp. Q3007–Q3011, Jan. 2016, doi: 10.1149/2.0021702jss.

[8] H. Machida, K. Hoshikawa, and T. Fukuda, "Growth of TiO_2 ribbon single crystals by edge-defined film-fed growth method," *J. Cryst. Growth*, vol. 128, nos. 1–4, pp. 829–833, Mar. 1993, doi: 10.1016/s0022-0248(07)80053-4.

[9] A. Kuramata, K. Koshi, S. Watanabe, Y. Yamaoka, T. Masui, and S. Yamakoshi, "High-quality β-Ga_2O_3 single crystals grown by edge-defined film-fed growth," *Jpn. J. Appl. Phys.*, vol. 55, no. 12, 2016, Art. no. 1202A2, doi: 10.7567/JJAP.55.1202A2.

[10] J. Yang, S. N. Ahn, F. Ren, S. J. Pearton, S. Jang, and A. Kuramata, "High breakdown voltage (-201) β-Ga_2O_3 Schottky rectifiers," *IEEE Electron Device Lett.*, vol. 38, no. 7, pp. 906–909, Jul. 2017, doi: 10.1109/LED.2017.2703609.

[11] J. Yang, S. Ahn, F. Ren, S. J. Pearton, S. Jang, J. Kim, and A. Kuramata, "High reverse breakdown voltage Schottky rectifiers without edge termination on Ga_2O_3," *Appl. Phys. Lett.*, vol. 110, no. 19, May 2017, Art. no. 192101, doi: 10.1063/1.4983203.

[12] K. Konishi, K. Goto, H. Murakami, Y. Kumagai, A. Kuramata, S. Yamakoshi, and M. Higashiwaki, "1-kV vertical Ga_2O_3 field-plated Schottky barrier diodes," *Appl. Phys. Lett.*, vol. 110, no. 10, Mar. 2017, Art. no. 103506, doi: 10.1063/1.4977857.

[13] C.-H. Lin, Y. Yuda, M. H. Wong, M. Sato, N. Takekawa, K. Konishi, T. Watahiki, M. Yamamuka, H. Murakami, Y. Kumagai, and M. Higashiwaki, "Vertical Ga_2O_3 Schottky barrier diodes with guard ring formed by nitrogen-ion implantation," *IEEE Electron Device Lett.*, vol. 40, no. 9, pp. 1487–1490, Sep. 2019, doi: 10.1109/led.2019.2927790.

[14] N. Allen, M. Xiao, X. Yan, K. Sasaki, M. J. Tadjer, J. Ma, R. Zhang, H. Wang, and Y. Zhang, "Vertical Ga_2O_3 Schottky barrier diodes with small-angle beveled field plates: A Baliga's figure-of-merit of 0.6 GW/cm^2," *IEEE Electron Device Lett.*, vol. 40, no. 9, pp. 1399–1402, Sep. 2019, doi: 10.1109/led.2019.2931697.

[15] W. Li, Z. Hu, K. Nomoto, R. Jinno, Z. Zhang, T. Q. Tu, K. Sasaki, A. Kuramata, D. Jena, and H. G. Xing, "2.44 kV Ga_2O_3 vertical trench Schottky barrier diodes with very low reverse leakage current," in *IEDM Tech. Dig.*, Dec. 2018, pp. 8.5.1–8.5.4, doi: 10.1109/iedm.2018.8614693.

[16] W. Li, Z. Hu, K. Nomoto, Z. Zhang, J. Hsu, Q. T. Thieu, K. Sasaki, A. Kuramata, D. Jena, and H. G. Xing, "1230 V β-Ga_2O_3 trench Schottky barrier diodes with an ultra-low leakage current of <1 μA/cm^2," *Appl. Phys. Lett.*, vol. 113, no. 20, 2018, Art. no. 202101, doi: 10.1063/1.5052368.

[17] S. J. Pearton, F. Ren, M. Tadjer, and J. Kim, "Perspective: Ga_2O_3 for ultra-high power rectifiers and MOSFETS," *J. Appl. Phys.*, vol. 124, no. 22, 2018, Art. no. 220901, doi: 10.1063/1.5062841.

[18] S. Nakagomi, K. Hiratsuka, Y. Kakuda, and Y. Kokubun, "Beta-gallium oxide/SiC heterojunction diodes with high rectification ratios," *ECS J. Solid State Sci. Technol.*, vol. 6, pp. Q3030–Q3034, Sep. 2017, doi: 10.1149/2.0061702jss.

[19] T. Watahiki, Y. Yuda, A. Furukawa, M. Yamamuka, Y. Takiguchi, and S. Miyajima, "Heterojunction p-Cu_2O/n-Ga_2O_3 diode with high breakdown voltage," *Appl. Phys. Lett.*, vol. 111, no. 22, Nov. 2017, Art. no. 222104, doi: 10.1063/1.4998311.

[20] J. Freitas, A. Kuramata, E. Glaser, A. Koehler, M. Tadjer, L. Luna, B. Feigelson, N. Mahadik, K. Hobart, and F. Kub, "Ga_2O_3 Schottky barrier and heterojunction diodes for power electronics applications," *Proc. SPIE, Gallium Nitride Mater. Devices*, vol. 10532, Feb. 2018, Art. no. 1053212, doi: 10.1117/12.2292211.

[21] Y. Kokubun, S. Kubo, and S. Nakagomi, "All-oxide p–n heterojunction diodes comprising p-type NiO and n-type β-Ga_2O_3," *Appl. Phys. Exp.*, vol. 9, no. 9, Sep. 2016, Art. no. 091101, doi: 10.7567/apex.9.091101.

[22] M. Grundmann, F. Klüpfel, R. Karsthof, P. Schlupp, F. Schein, D. Splith, C. Yang, S. Bitter, and H. Wenckstern, "Oxide bipolar electronics: Materials, devices and circuits," *J. Phys. D, Appl. Phys.*, vol. 49, no. 21, 2016, Art. no. 213001, doi: 10.1088/0022-3727/49/21/213001.

[23] M. Grundmann, R. Karsthof, and H. Von Wenckstern, "Interface recombination current in type II heterostructure bipolar diodes," *ACS Appl. Mater. Interfaces*, vol. 6, no. 17, pp. 14785–14789, Sep. 2014, doi: 10.1021/am504454g.